

# Comparison of Impurity Transport in Different Magnetic Configurations

Kieran J. McCarthy<sup>a</sup>, R. Burhenn<sup>b</sup>, K. Ida<sup>c</sup>, H. Maassberg<sup>b</sup>, Y. Nakamura<sup>c</sup>, N. Tamura<sup>c</sup>

<sup>a</sup> *Laboratorio Nacional de Fusión, Asociación EURATOM-CIEMAT, E-28040 Madrid, Spain*

<sup>b</sup> *Max-Planck-Institut für Plasmaphysik, EURATOM Association, D-17491 Greifswald, Germany*

<sup>c</sup> *National Institute for Fusion Science, 322-6 Oroshi-cho, Toki-shi, Gifu-ken 509-5292, Japan*

The goal of achieving steady state operation in stellarators brings into perspective the outstanding question of successful management of impurities, in particular, the avoidance of core impurity accumulation during improved energy confinement modes, with the resultant degradation of plasma energy due to radiation losses. Now, the dependence of impurity transport on plasma parameters has been systematically investigated during recent decades (LHD, W7-AS, TJ-II), in particular with regard to the influence of density and heating power on confinement. While certain global trends have been found in the different devices other behaviours are machine specific.

Here, after summarising the techniques for studying transport, we review transport observations under various stellarator plasma conditions in order to make comparisons, we draw attention to differing results for injected metallic and intrinsic impurities (core and edge), we identify those parameters that drive accumulation and discuss how observations compare with model predictions. Finally, in the light of results from LHD and W7-AS, we consider recent features such as the introduction of divertor modules in W7-AS that has allowed access to a high-density H-mode regime where radiation profiles reach a steady state, or the onset purification of LHD plasmas at higher density.

Keywords: Impurities, confinement, accumulation, transport,

## 1. Introduction

Impurities are an intrinsic component in fusion plasmas. Indeed, impurities are acceptable at low concentrations where they can be considered as being beneficial. For instance, impurities can provide a controlled manner to achieve radiative cooling at the plasma edge or their study, using spectroscopy, can provide essential information about the plasma edge or core. However, as we move towards advanced stellarators it has become imperative to avoid core impurity accumulation, in particular when operating in improved energy confinement modes, where accumulation (of high-Z impurities) can give rise to an overbalance of equilibrium between radiation losses and heating power with a resultant degradation of plasma energy and discharge termination.

The study of transport behaviour of intrinsic impurity ions in fusion plasmas is a long-standing field of research. Research on impurity accumulation and control remains a key issue in fusion research and is an indispensable part of ongoing investigations. In tokamaks, the appearance of, for example, edge-localized modes

(ELMs) (which also exist in stellarators but difficult to control) or sawtooth crashes, which originally are confinement-degrading phenomena, can be employed to clear out impurities. However, stellarators are free of externally induced currents and, consequently cannot utilize current-connected phenomena such as sawtoothing for impurity reduction. Moreover, owing to the existence of a magnetic topology that is quite different to that of tokamaks, additional transport regimes in the long-mean-free-path regime (lmfp) exist in stellarators<sup>1</sup> that might also affect impurity transport in the plateau or Pfirsch-Schlueter regime (*e.g.* the influence on temperature screening).

The continued study of impurity transport in stellarators is therefore fundamental, in particular, as the database in this area is smaller and less detailed than for tokamaks. A key question is to what extent observed impurity behaviour can be described by theoretical models developed for axisymmetric devices that nowadays have been adapted for stellarators, in particular, for the highly-collisional Pfirsch-Schlueter regime, where the difference between tokamak and stellarator is

assumed to be small. If good agreement with the theoretical model can be found, then the observed transport features are well understood and conclusions can be drawn with respect to further improvements and extrapolations. However, in the case of disagreement with theory, then this might point either to the domination of turbulent transport or the disregard of stellarator-specific transport contributions in the transport model. In this case, further interpretation becomes difficult and predictions have to be substituted by measurements. Depending on the collisionality regime of the impurities, the implementation of such non-axisymmetric effects self-consistently with the background plasma is an ambitious task and is not yet available for analysis.

In this paper, after a brief summary of theory and experimental techniques used for transport studies, we review transport observations under various stellarator plasma conditions in different stellarator devices in order to make comparisons, we then identify parameters that drive accumulation. We also consider recent features such as the introduction of divertor modules in W7-AS that has allowed access to a high-density H-mode regime where radiation profiles reach a steady state, or the onset purification of LHD plasmas at higher density, that may provide possible doorways to achieving improved management of impurities in long pulsed discharges. Finally, compare similarities and differences from the different configuration and we review database needs.

## 2. Background

At this point, it is useful to recall that the impurity influx into the plasma from the chamber walls, or other sources, is governed by transport at the open magnetic field and by retention whilst impurity transport inside the closed magnetic surface is governed by diffusive and convective terms. Indeed, impurity flux can be written simply in terms of diffusive and convective parts as

$$\Gamma = D \cdot \nabla n + v \cdot n \quad .$$

Here the convective part,  $v$ , is a strong function of ion temperature and density gradients, which for analysis purposes are often afflicted by certain errors depending on the profile quality, as well as by the collisionality regime of the background plasma. The diffusive part,  $D$ , may be considered less susceptible to error and better for comparisons.

Now, when the impurity ions are mostly in the highly collisional (Pfirsch-Schluter) regime it would be expected that the impurity transport in stellarators would be sufficiently decoupled from the magnetic topology so as to be similar to tokamaks. However, as stated before, the convective flux and its sign are determined by density and temperature gradients as well as the collisionality regime of the background plasma. For tokamaks with the

background plasma in the banana regime, this convective flux can be outward directed and helps to flush out impurities (“temperature screening”). In stellarators, however, additional collisionality regimes for the background gas appear in the  $lmfp$  region ( $v$ -,  $1/v$ -,  $v^{0.5}$ -regime) due to the 3-dimensional magnetic topology<sup>2</sup>. Unlike tokamaks, they are expected to lead to inward directed convective impurity fluxes (accumulation) also in the Pfirsch-Schluter collisionality regime for impurities. This would have important consequences for stellarators with respect to impurity radiation losses. Therefore, a comparison of experimental data with transport code predictions is a useful approach to elucidate the possible role of any neglected stellarator-specific aspects.

In order to study impurity transport several tools are available. On the experimental side, the monitoring of soft x-rays, from highly ionized high-Z impurities in the plasma core, or broadband radiation (using bolometers), is a common means of following impurity evolution. Moreover active tools are also available. These include laser blow-off, where a focused laser beam ablates a small amount of tracer material (typically a non-intrinsic metallic element) off a substrate, pellet injection where a micro-ball of material is accelerated to  $100^3 \text{ m s}^{-1}$  along a pipe-gun<sup>3</sup>, and gas oscillation. The tracer material released enters and traverses the plasma and the temporal behaviour of the different ionization states of the tracer ions in the plasma is monitored by spectrometers with central lines-of-sight. Thus, the impurity confinement time,  $\tau_{imp}$ , a global transport quantity, is derived from the temporal decay of the radiation emitted by the highest states. In order to extract local transport quantities across the plasma minor radius from such data, iterative procedures based on transport codes are employed. Similarly, the evolution of an intrinsic impurity can be evaluated by following the radiation emitted by highly ionized states and a model to reconstruct a steady-state solution of the charge-state distribution for the plasma with given density and temperature profiles. It should be noted here, that whilst the transport of intrinsic impurities is governed by transport both in the core and in the edge, impurity screening effects play no role in determining the transport of impurities injected using laser blow-off.

## 2. Experimental Impurity Transport

In this section we review results from a number of impurity transport experiments carried out for a range of plasma conditions in different stellarator machines. In most cases a short summary of the experiment is given and the most important results or findings are highlighted.

### 2.1 W7-AS

Electron cyclotron radiation (ECR)-heated plasmas

with a limiter configuration in W7-AS revealed a strong dependence of impurity confinement time on several plasma parameters, *i.e.*, on minor radius  $a_p$ , heating power  $P_{\text{ECRH}}$ , and plasma density  $n_e$  ( $\tau_{\text{Al}} \sim a_p^{2.4} n_e^{1.2} B^{0.3} / P_{\text{ECRH}}^{0.8}$ )<sup>4</sup>. See Fig. 1. Note: similar scalings were found for energy confinement and for particles<sup>5</sup>. The most important impact of this scaling on impurity transport with respect to consequences on machine performance is the unfavourable density dependence: at high densities (*e.g.*,  $7 \times 10^{19} \text{ m}^{-3}$ ), the confinement time reached values close to 1s or more. Stationary radiation levels could usually be sustained at low density without problems. However, beyond a central density of  $\sim 5 \times 10^{19} \text{ m}^{-3}$ , the intrinsic impurity radiation, as well as the  $Z_{\text{eff}}$ , started to rise continuously throughout the pulse length (see Fig. x, where all signals within the shaded region belong to discharges with densities  $> 5 \times 10^{19} \text{ m}^{-3}$ ). Thence, depending on the impurity flux level from the walls, this led to a degradation of plasma energy by excessive radiation losses.

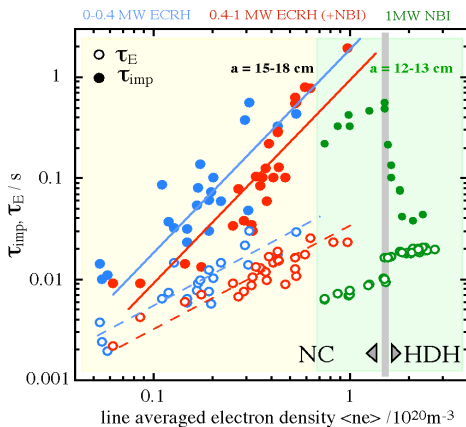


Fig.1. Energy and impurity confinement times vs. electron density for NC limiter ECRH plasmas (pink shaded region) and NBI plasmas (green shaded region) including the HDH transition during divertor operation. The gap between ECRH and NBI plasmas in the overlapping region is due to differences in the chosen plasma size.

These findings gave rise to several important questions. For instance, whether this effect was a consequence of changes in transport – as would be indicated by the long confinement times – or was the result of temporally increasing impurity sources from the wall (*e.g.* heating up of inboard tiles). This was investigated in an experiment using a constant fluorine gas puff ( $\text{CHF}_3$ ) applied throughout the pulse duration of a high-density discharge (Ref. 6) to simulate a stationary impurity source. The fluorine radiation in the plasma core rose continuously until the end of the pulse, this indicating an accumulation of fluorine in the core plasma. This supported the idea of a change of impurity transport

being responsible for the impurity accumulation at high density – rather than growing impurity source rates as a consequence of the heating up of inboard tiles.

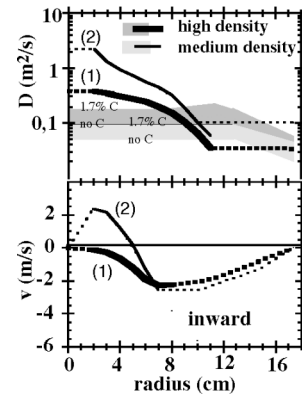


Fig.2. Transport coefficients for high ( $7 \times 10^{19} \text{ m}^{-3}$  (1)) and low density ( $3.5 \times 10^{19} \text{ m}^{-3}$  (2)) ECRH plasmas and model predictions (shaded area).

Another puzzling factor is the nearly missing dependence of the impurity confinement time on magnetic field strength  $B$  (*i.e.*  $\sim B^{0.3 (+/-0.2)}$ ). In order to elucidate two nearly identical plasmas with 1.25 and 2.5 T central magnetic field strengths were compared (Ref 6). It was revealed that the local impurity diffusion coefficient,  $D$ , in the plasma core was significantly higher ( $\times 3$  or  $4$ ) in the case of 1.25 T for radial positions with comparable densities. However, the inward convection  $v$  was also increased, so that, overall, the global impurity confinement time did not change. Although it is unclear whether this was a general characteristic, in the Pfirsch-Schluter regime,  $v$  may be directly related to  $D$  via some terms containing gradients in the background density and temperature profiles so the simultaneous increase of both transport coefficients may not contradict theory and may explain the unchanged confinement time.

It was also found that there was no electron temperature dependence. Furthermore, using laser blow-off into plasmas with different absolute densities, but very similar density profile shapes, it was found that the confinement time was not radial electric field dependent. This was further confirmed when comparing electric fields, as measured by charge-exchange, for different electron densities.

Now from a study comparing the intrinsic impurity radiation evolution in ECRH plasmas with different densities it was found that the different time behaviors of the intrinsic impurities could be explained by changes in transport alone<sup>7</sup>. For this, local transport coefficients were compared for a medium ( $3.5 \times 10^{19} \text{ m}^{-3}$ ) and a high ( $7 \times 10^{19} \text{ m}^{-3}$ ) central density discharge<sup>7</sup>. See Fig. 2. From analysis, it was seen that the centrally peaked  $D$  reduced by a factor  $\sim 2$  to  $3$  at high density whilst  $v$ 's were similar except in the centre where the differences with respect to

the large diffusion coefficients were considered of minor importance for overall confinement. It is interesting to remark here, that similarly peaked  $D$  profiles and density tendency were observed in the TJ-II, albeit at lower densities<sup>8</sup>. This brings up the question as to whether the peaked profiles in both devices are connected with ECRH deposition. This is a point for further investigation. Now, returning to W7-AS, model predictions (shaded areas) with different background impurity concentration assumptions suggests that the fast onset of a stationary radiation level can be well described by high-diffusive transport whilst the increase of radiation at high density was compatible with lower diffusion coefficients, in particular at the edge, where low diffusion coefficients govern the time constant for transport. Moreover, reduced impurity fluxes caused a longer time scale for achieving stationary conditions within the discharge duration (it was predicted that stationarity could be achieved after  $\sim 1.7$  s in the high density case)<sup>9</sup>. This is noteworthy as it implies that stationary radiation levels depend on impurity sources, i.e., small impurity sources may be acceptable for high-density plasmas. In such a case, wall conditioning comes to play an important role in accumulation prevention.

The scaling law also shows a degradation of impurity confinement with increased heating power. This was manifested by shorter decay times and by enhanced  $D$ 's, when laser blow-off was performed into plasmas with similar central densities, magnetic field strength and edge rotation transform but different injected ECRH power<sup>9</sup>. The difference in  $D$  was considered to be an indication for enhancement of turbulent transport at increased heating power in agreement with the observed power degradation of energy confinement. In contrast, the differences in  $v$  were relatively small. A degradation of impurity confinement with ECRH power ( $\tau \sim P^{-3}$ ) was found also in the TJ-II<sup>10</sup>. Indeed, it turned out to be stronger than the one observed in the global energy confinement ( $P^{0.6}$ ). Again, the manifestation of similar tendencies in different stellarator devices may be an indication of common underlying physics for impurity transport.

The investigation of impurity transport at densities higher than the ECRH cut-off frequency in W7-AS ( $1.2 \times 10^{20} \text{ m}^{-3}$ ) was restricted to neutral beam injection (NBI) heated plasmas. These were also characterized by long impurity confinement times, low diffusion coefficients and high inward convection. However, the previously observed density dependence on confinement, as well as the absolute values of transport coefficients, were not compatible with and often fell below neoclassical (and Pfirsch-Schlueter) predictions of the transport model for axisymmetric devices. Indeed,

differences in transport between H-mode and normal confinement-mode (NC) plasmas were difficult to extract because at higher densities where the H-mode usually appeared, the impurity confinement time of the NC plasma was already large.

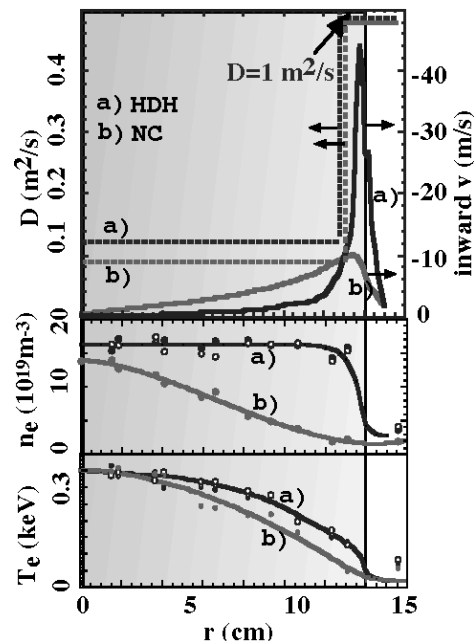


Fig.3. Top: transport coefficients for an HDH (a) and an NC (b) plasma with 1 MW NBI heating power. The shaded region is the confinement region of the plasma with separatrix around 14cm. bottom: density and temperature profiles of HDH and NC plasmas.

Finally, when operation with new island divertor modules began densities up to  $4 \times 10^{20} \text{ m}^{-3}$  were achieved<sup>11</sup>. Moreover, it was found that beyond a certain power dependent threshold density ( $1.5$  to  $2.1 \times 10^{20} \text{ m}^{-3}$ ), the unfavourable density scaling of impurity confinement in the NC regime changed suddenly. See Fig. 1. Within a narrow density interval, the plasma entered the High density H-mode regime where the impurity confinement time dropped by more than a magnitude to values comparable to the energy confinement time, which simultaneously increased by nearly a factor of 2<sup>12,13</sup>. As a result, quasi-stationary operation at densities up to  $4 \times 10^{20} \text{ m}^{-3}$  was possible.

The drop in impurity confinement in HDH was in agreement with the observed reduction of inward convection in the core (this being related to the flattening of the density profile) but is in contradiction to the strong inward convection at the plasma edge. Note; the temperature profile is very similar in both cases. Comparison with the H\*-mode, with nearly similar profiles to HDH but a large impurity confinement time, indicates the importance of edge transport. Now, in order to compensate for this large inward convection at the

plasma edge, a high edge diffusion pedestal is needed to achieve the short confinement times observed in HDH. See Fig. 3. This would highlight more the importance of the plasma edge for impurity transport.

## 2.II LHD

Impurity transport in the LHD device has been ongoing for several years. Indeed, both intrinsic and injected impurity transport has been studied in constant density and density ramp-up long pulse discharges (up to several 10's) heated by NBI<sup>14,15</sup>. One of the most notable findings has been the observation of intrinsic metallic accumulation in a narrow density window ( $\langle n_e \rangle \sim 1$  to  $3 \times 10^{19} \text{ m}^{-3}$ ) in hydrogen discharges. This was observed both for constant density and density ramp-up situations. In a constant density experiment, where the plasma density was kept almost constant at  $2.9 \times 10^{19} \text{ m}^{-3}$ , this core accumulation (the main metallic impurity being iron) manifested itself by an increase of central radiation power (the edge radiation power remaining almost constant) with a long timescale<sup>15</sup>. The increase in central radiation gave rise to a significant decrease in the central electron temperature. However, there was no radiation collapse of the plasma. In another experiment, with a slow density ramp-up, a dramatic alteration of impurity behaviour was observed. In the first instance, the central radiation increased rapidly with density. See Fig. 4. Then, as the density was increased further, the central radiation began to reduce steadily. From analysis of the evolution of the central radiation power and highly-ionised iron line emission evolutions using the one-dimensional impurity transport code (MIST)<sup>16</sup> an impurity accumulation window was deduced. Here, the central iron density increased steadily when  $\langle n_e \rangle$  was above  $\sim 10^{19} \text{ m}^{-3}$ , reaching a peak at about  $\langle n_e \rangle \sim 2.7 \times 10^{19} \text{ m}^{-3}$ . When the plasma density increased beyond this density turning point the central iron

density fell off, this being interpreted as impurity clear- or flush-out processes. In another similar study, it was also found that accumulation could be avoided in this accumulation window by performing a fast density ramp-up. It was then found that metallic impurities would not accumulate as they passed through the accumulation window before accumulation could occur.

In order to further understand this impurity behaviour, radial electric field profiles,  $E_r$ , derived from poloidal rotation velocity measurements made using charge exchange spectroscopy of neon, were also considered<sup>17</sup>. It was found that  $E_r$  near the plasma edge changed from positive (electron root) to negative (ion root) as density increased, the transition occurring near the density where the accumulation window begins ( $10^{19} \text{ m}^{-3}$  with  $T_i \sim 2 \text{ keV}$ ). Indeed in LHD where the density profile is flat in the core and the temperature profile is almost parabolic for discharges maintained with gas puffing, it was determined that the impurity flux is determined by the convection velocity for the metallic impurities. In the region of high temperature and low density, high-Z accumulation was avoided due to this positive  $E_r$ , towards the edge. In the high density and low temperature region (high collisionality), accumulation was not seen, this being attributed to the dominant contribution of the temperature gradient in the PS regime (temperature screening effect). Here, the qualitative behaviour of neon penetration into the plasma core could be accounted for by a large convection contribution due to the radial electric field, this being explained from neoclassical impurity transport for the  $v^{-1}$  regime for a nonaxisymmetric which predicted a large convective component proportional to  $E_r$ . On the whole, the qualitative features were considered consistent with neoclassical impurity transport. However, the inward impurity flux (accumulation) is not found in a simple analysis with neoclassical theory, even when including an expression for axisymmetric torus plasmas.

Pellet injection experiments using titanium have also been performed for a range of constant density plasmas<sup>18</sup>. At low density, the titanium exited the plasma and there was no accumulation. Furthermore, the associated Ti emission decay time, which is closely connected to impurity confinement time, could be explained by the diffusion component only in an impurity transport analysis. At higher density, an abrupt increase in the Ti emission decay time was observed right across the accumulation window region implying long confinement. Indeed, it is not unrealistic to consider that the impurity confinement time could continue to increase when above the accumulation window density region. Moreover, if the  $\tau$  and  $E_r$  were to continue to rise at high density, then the purification window would mean that there is a decrease of impurity influx but still long

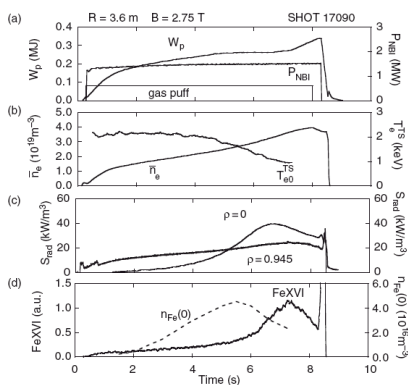


Figure 6. Time evolution of plasma parameters and the central iron density in a density ramp-up discharge (Shot 17090). The plasma density increases with time by constant gas puffing. The central iron density was estimated with the impurity transport code MIST.

Fig. 4. Time evolution of LHD plasma parameters and central iron density in a density ramp-up discharge.

confinement times. If so then this may be similar to HDH on W7-AS.

### 3. Similarities and Differences

In summary, there are indications for anomalous/turbulent transport at low and medium densities in all machines and a tendency to approach neoclassics at high density. In addition, it has been indicated that there is an improvement of impurity core confinement with increasing density. Moreover, it is important to determine if impurity screening mechanisms at high density are similar or not in W7-AS and LHD. Indeed, many features are qualitatively consistent with traditional neoclassics but not quantitatively consistent with traditional neoclassics. Finally there is a need to implement non-axisymmetric neoclassical theory in order to achieve a better understanding of the underlying physics.

### 4. Database

For an impurity transport database, new data, or the systematic reviewing and cataloguing of existing data, are required in order to improve scaling laws for the different machines. For instance, this might include the influence on  $\tau_{\text{imp}}$  of magnetic field strength, density, temperature,  $\iota$ , heating power and type, radial electric field. Furthermore, diffusion and convective coefficients at 2 or more radial points would also be needed in order to evaluate the contribution of local transport. Furthermore, such data would help to achieve a better understanding of the physics of impurity transport and aid comparison. Also, in order to attain a basis for better understanding it will be necessary to consider stellarator specific features in neoclassical models, for instance, 3-D magnetic topology, gradB-drift, *etc.* Finally, a crucial point for future predictions will be to determine when can impurity transport be described by a neoclassical model and when is it anomalous or turbulent.

### Acknowledgements

This work contributes to the International Stellarator Profile Database under the auspices of the IEA Implementing Agreement for Cooperation in the Development of the Stellarator Concept. The authors acknowledge the contributions of the W7-AS, LHD and TJ-II teams to this work.

### References

- [1] A.A Galeev and R.Z. Sagdeev, Reviews of Plasma Physics, Vol. 7, M.A. Leontovich, Ed. Consultants Bureau, New York (1979).
- [2] H. Maassberg et al., Plasma Phys. Control. Fusion 41, 1135 (1999).
- [3] S. Sudo et al., Plasma Phys. Control. Fusion 44, 129 (2002).
- [4] R. Burhenn et al., Proc. 22nd Conf. Controlled Fusion and Plasma Physics, Bournemouth, United Kingdom,

- 1995, Europhysics Conference Abstracts, Vol. 19C, Part III, p. 145, European Physical Society-
- [5] U. Stroth et al., Nucl. Fusion 36, 8 (1996).
- [6] R. Burhenn et al., Proc. 27th Conf. Controlled Fusion and Plasma Physics, Budapest, Hungary, 2000, Europhysics Conference Abstracts, Vol. 24B, Part 3.041, European Physical Society.
- [7] R. Burhenn et al., Proc. 24th Conf. Controlled Fusion and Plasma Physics, Berchdesgaden, Germany, 1997, Europhysics Conference Abstracts, Vol. 21A, Part IV, p.1609, European Physical Society.
- [8] B. Zurro et al., Rev. Sci. Instrum. 75, 10 (2004)
- [9] R. Burhenn et al. Fusion Sci. Tech. 46, 115 (2004).
- [10] C. Hidalgo et al., Nucl. Fusion 45, S266 (2005).
- [11] P. Grigull et al., Fusion Eng. Design 66-68, 49 (2003).
- [12] K. McComick et al., Phys. Rev. Lett. 89,015001-1 (2002).
- [13] R.R. Jaenicke et al., Plasma Phys. Control. Fusion 44B, 193 (2002).
- [14] Y. Nakamura et al. Nucl. Fusion 43, 219 (2003).
- [15] Y. Nakamura et al., Plasma Phys. Control. Fusion 44, 2121 (2002).
- [16] R.A. Hulse, Nucl. Tech./Fusion 3, 259 (1983).
- [17] K. Ida et al., Rev. Sci. Instrum. 71, 2360 (2001).
- [18] N. Tamura et al., Plasma Phys. Control. Fusion 45, 27 (2003).